

Characterization of Store-operated Ca^{2+} Entry in 3T3-L1 Cells

Chikara OTSUBO^{1,4}, Osamu TERASAKA², Takashi UDAGAWA^{1,3}, and Masahiro KAWAMURA¹

¹*Department of Pharmacology, The Jikei University School of Medicine*

²*Division of Biology, The Jikei University School of Medicine*

³*Division of Kidney and Hypertension, Department of Internal Medicine, The Jikei University School of Medicine*

⁴*Department of Pediatrics, The Jikei University School of Medicine*

ABSTRACT

3T3-L1 preadipocytes differentiate into mature adipocytes and are useful for studying the mechanism of obesity. The mobilization of intracellular Ca^{2+} concentration ($[\text{Ca}^{2+}]_i$) is related to adipocyte differentiation. Therefore, we studied the mechanisms regulating $[\text{Ca}^{2+}]_i$ mobilization in isolated fura-2-loaded 3T3-L1 preadipocytes. Thapsigargin and prostaglandin $\text{F}2\alpha$ ($\text{PGF}2\alpha$) are known to cause Ca^{2+} influx from the extracellular space. However, this influx was inhibited by 2 store-operated Ca^{2+} entry (SOCE) inhibitors: 2-aminoethoxydiphenyl borate and Ni^{2+} . These results indicated the presence of a SOCE system in 3T3-L1 preadipocytes. Although the actin cytoskeleton plays an important role in many cell functions, whether the actin network affects SOCE remains controversial. Cytochalasin D, an actin-depolymerizing agent, and calyculin A, a cortical actin-reorganizing agent, did not inhibit thapsigargin-induced $[\text{Ca}^{2+}]_i$ mobilization. These results suggested that the actin cytoskeleton does not participate in SOCE in 3T3-L1 preadipocytes. Canonical transient receptor potential channels (TRPs) have recently been reported to be involved in SOCE. We detected TRPC1 and TRPC2 messenger RNAs by reverse transcriptase polymerase chain reaction. However, we did not observe Sr^{2+} influx. Therefore, we inferred that TRPCs do not take part in SOCE in 3T3-L1 preadipocytes.

(Jikeikai Med J 2010; 57: 43-53)

Key words: calcium, store-operated Ca^{2+} entry, cytoskeleton, preadipocyte

INTRODUCTION

Obesity is a major risk factor for hypertension, heart diseases, and diabetes. Furthermore, increasing adipose tissue results in obesity. Therefore, the adipogenic mechanism of preadipocytes has been extensively studied. In many studies, 3T3-L1 preadipocytes, which differentiate into adipocytes under appropriate conditions, are often used as an *in vitro* model.

Ca^{2+} is an important regulator of various intracellular events. Intracellular mobilization of Ca^{2+} con-

trols many cellular functions, including proliferation, transcription, differentiation, and apoptosis¹. The process of adipocyte differentiation is affected by the mobilization of intracellular Ca^{2+} concentration ($[\text{Ca}^{2+}]_i$) in 3T3-L1 preadipocytes.

Nakada et al. have reported that prostaglandin $\text{F}2\alpha$ ($\text{PGF}2\alpha$) increases intracellular Ca^{2+} concentration ($[\text{Ca}^{2+}]_i$) in 3T3-L1 preadipocytes². There are $\text{PGF}2\alpha$ receptors (FP receptors) in 3T3-L1 preadipocytes³. However, the precise system involved in cytosolic Ca^{2+} mobilization in 3T3-L1 cells remains unclear. Ca^{2+} enters the cells from the extracellular

Received for publication, May 27, 2009

大坪 主税, 寺坂 治, 宇田川 崇, 川村 将弘

Mailing address: Chikara OTSUBO, Department of Pediatrics, The Jikei University School of Medicine, 3-25-8, Nishi-Shimbashi, Minato-ku, Tokyo 105-8461, Japan.

E-mail: konikatsubooh04@jikei.ac.jp

space through various types of Ca^{2+} entry systems (i.e., voltage-operated Ca^{2+} channel, receptor-operated Ca^{2+} channel, and store-operated Ca^{2+} entry [SOCE])⁴. Therefore, we investigated the Ca^{2+} entry system that uses $\text{PGF}2\alpha$ and how the ion is transported into the 3T3-L1 cells.

MATERIALS AND METHODS

1. Cell culture and adipocyte differentiation

3T3-L1 preadipocytes were obtained from the American Type Culture Collection (Manassas, VA, USA) and cultured in Dulbecco's modified Eagle's medium (DMEM) supplemented with 10% calf serum, 100 U/mL penicillin, and 100 $\mu\text{g}/\text{mL}$ streptomycin at 37°C in a humidified atmosphere with 5% CO_2 .

Two days after the cells reached confluence (day 0), adipocyte conversion was induced with 0.25 μM dexamethasone, 0.5 mM 3-isobutyl-1-methylxanthine, and 1 $\mu\text{g}/\text{mL}$ insulin in DMEM supplemented with 10% fetal calf serum. After 2 days (day 2), the culture medium was replaced with DMEM supplemented with 10% fetal calf serum and 1 $\mu\text{g}/\text{mL}$ insulin. The medium was changed every other day with DMEM supplemented with 10% fetal calf serum. After 10 days (day 10), 3T3-L1 preadipocytes differentiated into adipocytes (3T3-L1 adipocytes). Adipocyte differentiation was confirmed by Oil Red O staining.

2. Measurement of $[\text{Ca}^{2+}]_i$

Isolated 3T3-L1 cells were loaded with 2 μM fura-2/acetoxymethyl ester (fura-2/AM) in Krebs-Ringer HEPES buffer (123 mM NaCl, 4.6 mM KCl, 1.2 mM KH_2PO_4 , 1.2 mM MgSO_4 , 1.2 mM CaCl_2 , 11.1 mM glucose, 0.1% bovine serum albumin, and 10 mM HEPES, pH 7.4) for 30 minutes at 37°C. The cells were centrifuged and resuspended in the above buffer and incubated for further 30 minutes at 37°C to allow hydrolysis of the intracellular fura-2 ester. Fluorescence of the fura-2 loaded cells was monitored using a fluorescence spectrophotometer (F-2000, Hitachi Medical Corporation, Tokyo, Japan) at 25°C with continuous stirring at an emission wavelength of 510 nm and excitation wavelengths of 340 and 380 nm. The $[\text{Ca}^{2+}]_i$ was indicated by the ratio of the fluores-

cence intensity at the 340-nm excitation wavelength to that at 380 nm (I340/I380)⁵.

3. Fluorescent staining of filamentous actin

Fluorescent staining of filamentous actin (F-actin) was monitored as previously described⁶. Briefly, 3T3-L1 preadipocytes cultured on a coverslip were fixed in 10% formaldehyde at room temperature. The fixed cells were permeabilized with 0.1% Triton-X, followed by incubation with rhodamine-phalloidin. Fluorescent images were observed with a microscope (Microphoto-FX, Nikon Corp., Tokyo, Japan) and photographed (Kodak Tri-X Pan film, Eastman Kodak Co., Rochester, NY, USA).

4. Reverse transcriptase polymerase chain reaction for canonical transient receptor potential proteins

The reverse transcription (RT) reaction was performed with the SuperScript II 1st Strand DNA Synthesis Kit (Invitrogen Corp., Carlsbad, CA, USA) followed by 50 cycles of polymerase chain reaction (PCR) (1 minute at 94°C, 1 minute at 54.4°C, and 2 minutes at 72°C). Specific primers for canonical transient receptor potential channels (TRPs)¹⁻⁷ were as follows^{7,8}: murine (m) TRPC1, forward 5'-GATTTTGGGAAATTTCTGGG-3', reverse 5'-TGTTATCAGCTGGAAGCT-3'; mTRPC2, forward 5'-GACATGATCCGGTTCATG-3', reverse 5'-CTGGATCTTCTGGAAGGA-3'; mTRPC3, forward 5'-GACATATCAAGTTCATGGT-3'; reverse, 5'-CTGGATCTCTTGGTATGA-3'; mTRPC4, forward 5'-TGGGACATGTGGCACCCAC-3', reverse 5'-ACGTGGAAAACGCGTTGTTCTG-3'; mTRPC5, forward 5'-GACTAGTCTTGATATACTCAAATTTCTC-3', reverse 5'-GGGGTACCTCAGCATGATGGCAATG-3'; mTRPC6, forward 5'-GATATCTTCAAATTCATGGTC-3', reverse 5'-CTCAATTTCTGGAATGAAC-3'; mTRPC7, forward 5'-TGTAACGCTGCACAACGTCTCA-3', reverse 5'-AATTCCTCATGCCAGCCTGGTA-3'. The expected lengths of amplified fragments were 356, 297, 309, 304, 365, 309, and 767 base pairs for mTRPC1, mTRPC2, mTRPC3, mTRPC4, mTRPC5, mTRPC6, and mTRPC7, respectively^{7,8}.

5. Statistical analysis

Statistical analysis was performed by analysis of variance. The level of statistical significance was set at $P < 0.05$.

6. Reagents

The reagents were purchased from the following companies: fura-2/AM from Dojindo Laboratories (Kumamoto, Japan); thapsigargin, PGF2 α , 3-isobutyl-1-methylxanthine, insulin, dexamethasone, cytochalasin D, and calyculin A from Sigma-Aldrich Co., (St. Louis, MO, USA); 2-aminoethoxydiphenyl borate (2-APB) from Tokyo Chemical Industry Co., (Tokyo, Japan); and DMEM from Invitrogen Co., (Carlsbad, CA, USA). All the other chemicals were of reagent grade.

RESULTS

1. Effects of PGF2 α and thapsigargin on $[Ca^{2+}]_i$ mobilization in 3T3-L1 preadipocytes

PGF2 α (1 μ M) brought about a two-phase increase of $[Ca^{2+}]_i$ in the presence of extracellular Ca^{2+} . The first phase was rapid and transient, and the second phase was a sustained rise (Fig. 1A (a)). However, in the absence of extracellular Ca^{2+} , the phase was significantly reduced (Fig. 1A (a)). In the absence of extracellular Ca^{2+} , the difference between the ratios at 600 sec and at the beginning of the determination was significantly lower in PGF2 α -treated cells than in control cells ($P < 0.001$) (Fig. 1A (b)). PGF2 α binds to FP receptor-coupled Gq protein and activates phospholipase C, resulting in inositol 1, 4,5-trisphosphate (IP3)-stimulated Ca^{2+} release from the endoplasmic reticulum (ER) to deplete luminal Ca^{2+} ^{9,10}. The depletion of luminal Ca^{2+} in the ER

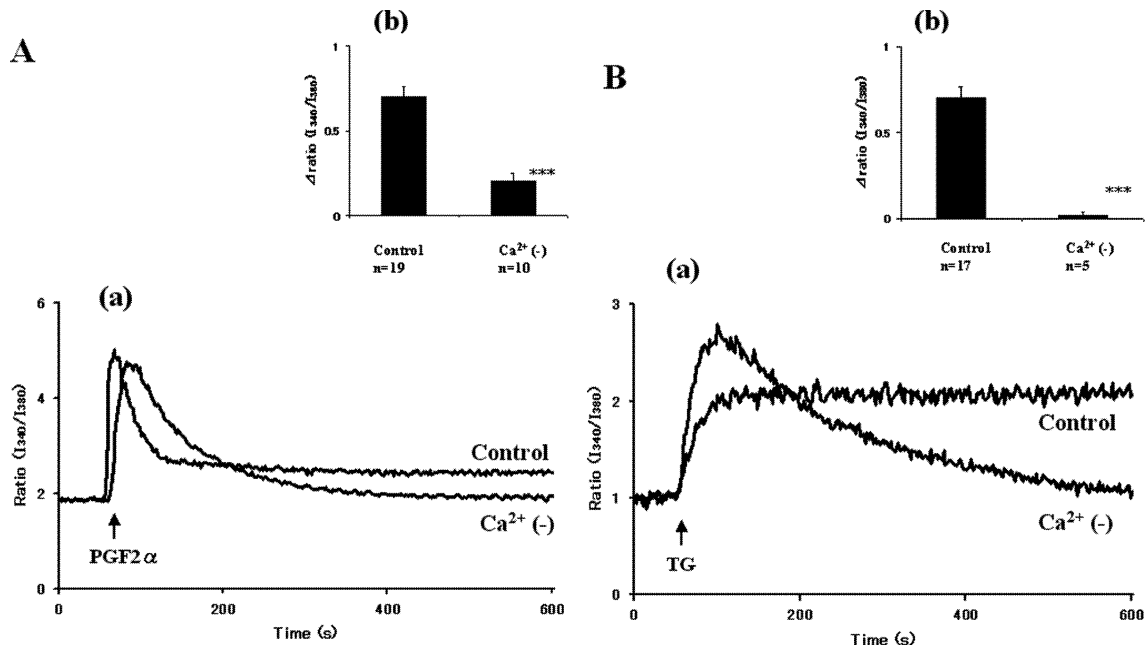


Fig. 1. Effects of PGF2 α and thapsigargin on $[Ca^{2+}]_i$ mobilization in 3T3-L1 preadipocytes. PGF2 α (1 μ M) and thapsigargin (2 μ M) were added 50 seconds after the beginning of fluorescence determination in the presence or absence of extracellular Ca^{2+} (1.2 mM). A (a): Effect of PGF2 α on $[Ca^{2+}]_i$ mobilization in 3T3-L1 preadipocytes. Typical tracings are shown. A (b): The difference between the ratios of I340/I380 at 600 seconds and at the beginning of fluorescence determination in the presence and absence of extracellular Ca^{2+} . B (a): Effect of thapsigargin on $[Ca^{2+}]_i$ mobilization in 3T3-L1 preadipocytes. Typical tracings are shown. B (b): The difference between the ratios of I340/I380 at 600 seconds and at the beginning of fluorescence determination in the presence and absence of extracellular Ca^{2+} . Each value represents the mean \pm S.E.; ***, $P < 0.001$.

triggers Ca^{2+} influx from the extracellular space. To examine this possibility, we investigated the effect of thapsigargin, which depletes luminal Ca^{2+} in the ER by the inhibiting Ca^{2+} -ATPase of ER¹¹.

Thapsigargin (1 μM) caused a rapid increase and a sustained phase of fura-2-fluorescence intensity in the presence of extracellular Ca^{2+} (1.2 mM) (Fig. 1B (a)). However, in the absence of extracellular Ca^{2+} , the sustained phase was abolished (Fig. 1B (a)).

In the absence of extracellular Ca^{2+} , the difference between the ratio at 600 sec and that at the beginning of the determination was significantly lower in thapsigargin-treated cells, than in control cells

($P < 0.001$) (Fig. 1B (b)).

The results indicated that the first rapid increase phase was due to Ca^{2+} release from the ER and that the sustained phase was due to Ca^{2+} entry from the extracellular space.

2. Effects of 2-APB and Ni^{2+} on $\text{PGF}2\alpha$ - and thapsigargin-induced $[\text{Ca}^{2+}]_i$ mobilization in 3T3-L1 preadipocytes

As shown in Figure 2A (a) and B (a), 2-APB (100 μM) and Ni^{2+} (1 mM) significantly reduced the second phase induced by $\text{PGF}2\alpha$. These inhibitory effects of 2-APB and Ni^{2+} were significantly lower than the

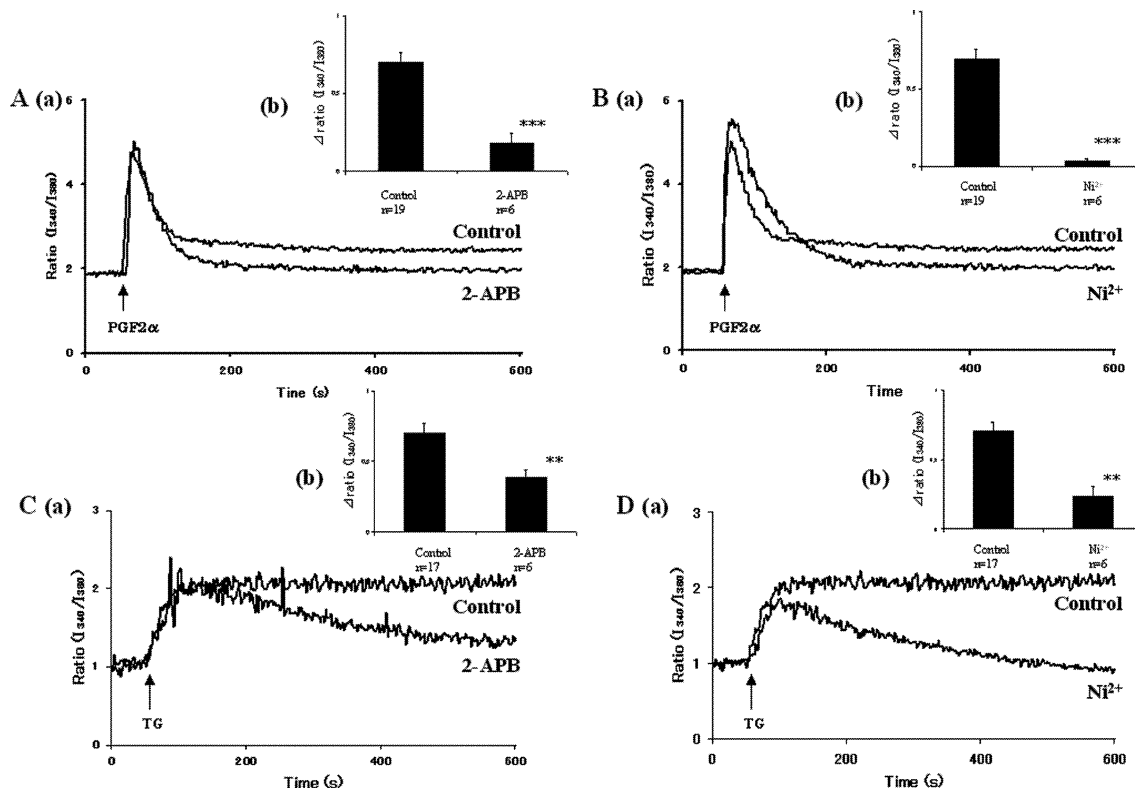


Fig. 2. Effects of 2-APB and Ni^{2+} on $\text{PGF}2\alpha$ - and thapsigargin-induced $[\text{Ca}^{2+}]_i$ mobilization in 3T3-L1 preadipocytes. Cells were pretreated with 2-APB (100 μM) or Ni^{2+} (1 mM) before the addition of $\text{PGF}2\alpha$ (1 μM) and thapsigargin (2 μM). A (a): Effect of 2-APB on $\text{PGF}2\alpha$ -induced $[\text{Ca}^{2+}]_i$ mobilization in 3T3-L1 preadipocytes. Typical tracings are shown. A (b): The difference between the ratios of I340/I380 at 600 seconds and at the beginning of fluorescence determination. B (a): Effect of Ni^{2+} on $\text{PGF}2\alpha$ -induced $[\text{Ca}^{2+}]_i$ mobilization in 3T3-L1 preadipocytes. Typical tracings are shown. B (b): The difference between the ratios of I340/I380 at 600 seconds and at the beginning of fluorescence determination. C (a): Effect of 2-APB on thapsigargin-induced $[\text{Ca}^{2+}]_i$ mobilization in 3T3-L1 preadipocytes. Typical tracings are shown. C (b): The difference between the ratios of I340/I380 at 600 seconds and at the beginning of the fluorescence determination. D (a): Effect of Ni^{2+} on thapsigargin-induced $[\text{Ca}^{2+}]_i$ mobilization in 3T3-L1 preadipocytes. Typical tracings are shown. D (b): The difference between the ratios of I340/I380 at 600 seconds and at the beginning of fluorescence determination. Each value represents the mean \pm S.E.; ***, $P < 0.001$. **, $P < 0.01$.

control value ($P < 0.001$) (Fig. 2A (b) and B (b)). 2-APB and Ni^{2+} also attenuated the thapsigargin-induced sustained phase (Fig. 2C (a) and D (a)). Their inhibitory effects were significantly lower than the control value ($P < 0.01$) (Fig. 2C (b) and D (b)). These results confirm that SOCE is involved in $\text{PGF}2\alpha$ - and thapsigargin-induced Ca^{2+} entry.

3. Effects of cytochalasin D and calyculin A on thapsigargin-induced $[\text{Ca}^{2+}]_i$ mobilization in 3T3-L1 preadipocytes

Pretreatment with $10 \mu\text{M}$ cytochalasin D15 for 1 hour did not alter thapsigargin-induced $[\text{Ca}^{2+}]_i$ mobilization (Fig. 3A (a)). Moreover, under the present experimental conditions, pretreatment with calyculin A (100 nM , 30 minutes) did not alter the plateau phase evoked by thapsigargin in 3T3-L1 preadipocytes (Fig. 3B (a)). The difference between the ratios of I340/I380 at 600 seconds and at the beginning of fluorescence determination in cytochalasin D- and calyculin A-

treated cells was not significantly lower than in the control (Fig. 3A (b) and B (b)).

4. Effects of cytochalasin D and calyculin A on the actin network in 3T3-L1 preadipocytes

As shown in figure 4, F-actin was visible under a confocal microscope after rhodamine-phalloidin staining. Rhodamine-phalloidin staining showed F-actin fibers distributed parallel or perpendicular to each other in the control cells (Fig. 4A). In the cells treated with cytochalasin D ($10 \mu\text{M}$, 1 hour), no stress fibers were seen, and depolymerized actin converted into bundles (Fig. 4B). After treatment with calyculin A (100 nM , 30 minutes), F-actin redistributed to the cell periphery to create the dense phase (Fig. 4C).

5. Expression of TRPC mRNA by RT-PCR in 3T3-L1 preadipocytes

Expression of TRPC1 and TRPC2 mRNA was detected after 50 PCR cycles in 3T3-L1 preadipocytes

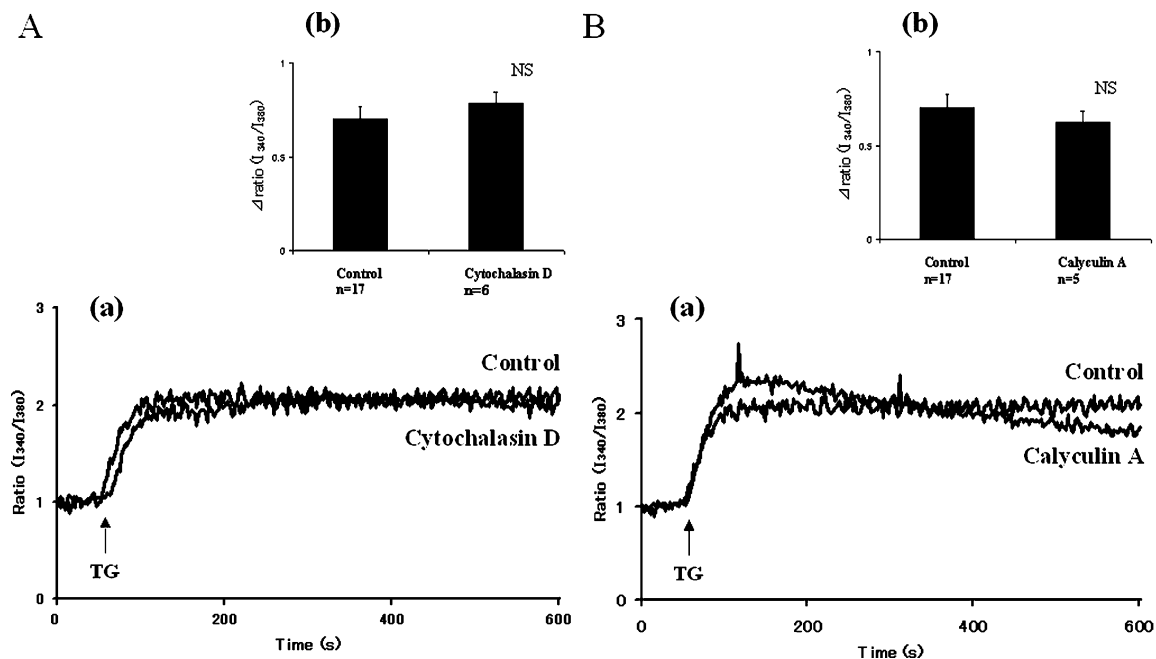


Fig. 3. Effects of cytochalasin D and calyculin A on thapsigargin-induced $[\text{Ca}^{2+}]_i$ mobilization in 3T3-L1 preadipocytes. Cells were pretreated with cytochalasin D ($10 \mu\text{M}$) for 1 hour and with calyculin A (100 nM) for 30 minutes before the addition of thapsigargin ($2 \mu\text{M}$). A (a): Effect of cytochalasin D on thapsigargin-induced $[\text{Ca}^{2+}]_i$ mobilization in 3T3-L1 preadipocytes. Typical tracings are shown. A (b): The difference between the ratios of I340/I380 at 600 seconds and at the beginning of fluorescence determination. B (a): Effect of calyculin A on thapsigargin-induced $[\text{Ca}^{2+}]_i$ mobilization in 3T3-L1 preadipocytes. Typical tracings are shown. B (b): The difference between the ratios of I340/I380 at 600 seconds and at the beginning of fluorescence determination. Each value represents the mean \pm S.E.; NS, not significantly different.

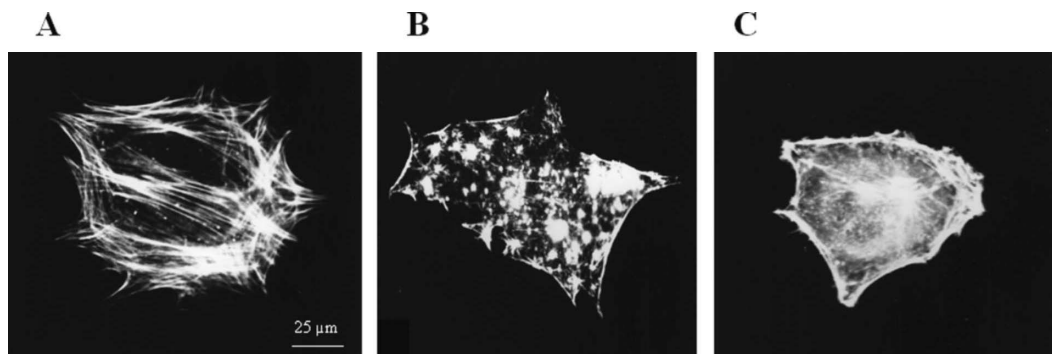


Fig. 4. Effects of cytochalasin D and calyculin A on the actin network in 3T3-L1 preadipocytes. (A) Control ; (B) Treated with 10 μ M cytochalasin D for 1 hour ; (C) Treated with 100 nM calyculin A for 30 minutes



Fig. 5. Expression of TRPC mRNA by RT-PCR in 3T3-L1 preadipocytes. RT-PCR of cDNA was performed using the specific primers shown under Materials and Methods. M: markers.

(Fig. 5). No other TRPC mRNAs were detected (data not shown).

6. *PGF2 α - and thapsigargin-induced fura-2 fluorescence intensity in the presence of extracellular Sr²⁺ in 3T3-L1 preadipocytes*

Under these conditions, the plateau phases induced by *PGF2 α* and thapsigargin were attenuated (Fig. 6A (a) and B (a)). In the presence of extracellular Sr²⁺, the differences between the ratios of I340/I380 at 600 seconds and at the beginning of fluorescence determination were significantly lower than the control value ($P < 0.001$) (Fig. 6A (b) and B (b)).

7. *PGF2 α - and thapsigargin-induced [Ca²⁺]_i mobilization in 3T3-L1 preadipocytes and 3T3-L1 adipocytes*

The *PGF2 α -* and thapsigargin-induced sustained phases in 3T3-L1 adipocytes were similar to those induced in 3T3-L1 preadipocytes (Fig. 7A (a) and B (a)). The differences between the ratios of I340/I380 at 600 seconds and at the beginning of the fluorescence determination did not differ significantly between adipocytes and preadipocytes (Fig. 7A (b) and B (b)).

DISCUSSION

1. *SOCE in 3T3-L1 preadipocytes*

Ca²⁺ is one of the most important messengers of various cellular functions, such as proliferation, differentiation, gene transcription, and apoptosis¹. Previous studies have shown that in 3T3-L1 preadipocytes, the increase in [Ca²⁺]_i affects adipocyte differentiation²¹. However, the details of [Ca²⁺]_i mobilization in 3T3-L1 cells are unclear. At least 3 types of Ca²⁺ channel regulate Ca²⁺ entry across the plasma membrane: the voltage-operated Ca²⁺ channel, the receptor-operated Ca²⁺ channel, and the SOCE channel⁴. In this study, a high K⁺ concentration failed to trigger Ca²⁺ influx into 3T3-L1 preadipocytes (data not shown). However, Ca²⁺ store depletion from the ER by *PGF2 α -* and thapsigargin induced Ca²⁺ influx. In addition, SOCE inhibitors 2-APB and Ni²⁺ abolished *PGF2 α -* and thapsigargin-induced Ca²⁺ entry. These results indicated that 3T3-L1 preadipocytes possess SOCE but not voltage-

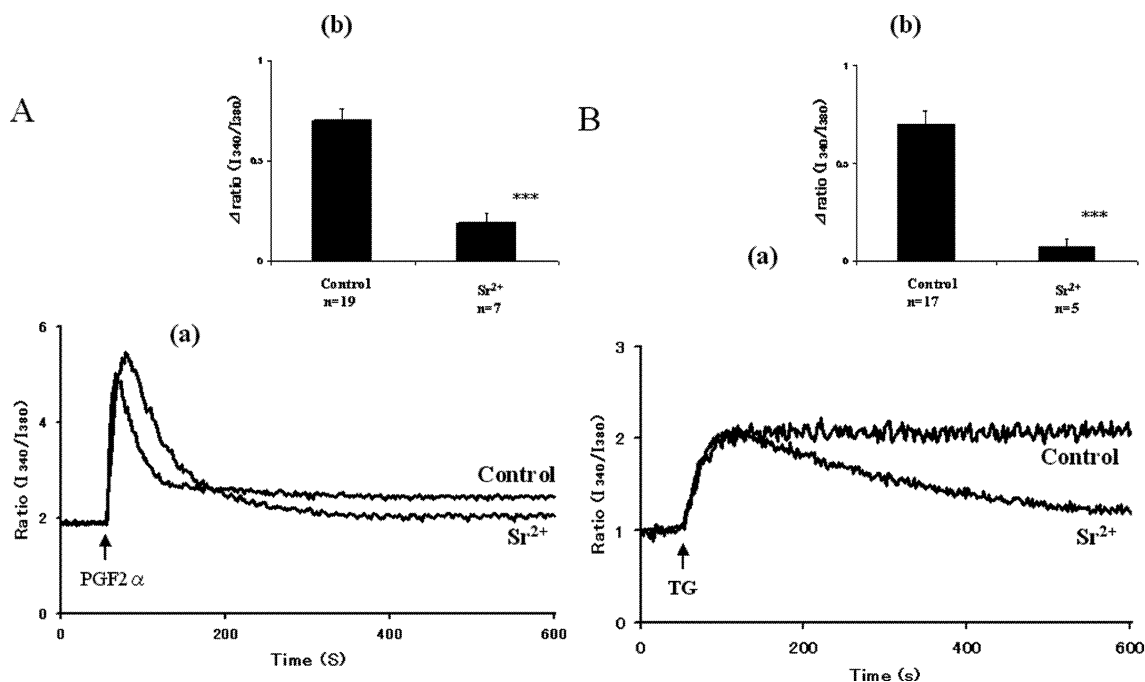


Fig. 6. PGF2 α - and thapsigargin-induced fura-2 fluorescence intensity in the presence of extracellular Sr²⁺ in 3T3-L1 preadipocytes. The 1.2 mM Ca²⁺ in the incubation buffer (control) was replaced with 1.2 mM Sr²⁺ (Sr²⁺). A (a): Effect of PGF2 α -induced fura-2-fluorescence intensity in the presence of extracellular Sr²⁺ in 3T3-L1 preadipocytes. Typical tracings are shown. A (b): The difference between the ratios of I340/I380 at 600 seconds and at the beginning of fluorescence determination. B (a): Effect of thapsigargin-induced fura-2-fluorescence intensity in the presence of extracellular Sr²⁺ in 3T3-L1 preadipocytes. Typical tracings are shown. B (b): The difference between the ratios of I340/I380 at 600 seconds and at the beginning of fluorescence determination. Each value represents the mean \pm S.E.; ***, $P < 0.001$.

operated Ca²⁺ channels.

Three mechanisms of SOCE have been hypothesized: a conformational coupling model, a vesicular fusion model, and a diffusible messenger model. In the conformational coupling model, the ER moves to the plasma membrane after luminal Ca²⁺ store depletion by IP₃ via the IP₃ receptor in the ER²²⁻²⁵. The vesicular fusion model suggests that upon Ca²⁺ store depletion, vesicles containing SOCE channels fuse with the plasma membrane, and SOCE is activated¹⁸. In the diffusible messenger model, SOCE is activated by the diffusible messenger that is produced upon Ca²⁺ store depletion²⁶. Among these models, the conformational coupling model and the vesicular fusion model might be closely related to the dynamics of the actin cytoskeleton.

We examined whether the actin cytoskeleton was involved in SOCE in 3T3-L1 preadipocytes. Phase-contrast microscopy revealed that the actin filaments were distributed primarily throughout the cytoplasm

in the control cells. After 1 hour of treatment with cytochalasin D, actin filaments became depolymerized. Pretreatment with calyculin A caused reconstruction of the actin filaments in the cell periphery. The conformational coupling model proposes that Ca²⁺ store depletion causes the ER to move towards the plasma membrane to facilitate coupling between the IP₃ receptor and the SOCE channel. The actin cytoskeleton is related to SOCE between the ER and the plasma membrane. In spite of the gross structural changes in the actin cytoskeleton after treatment with cytochalasin D and calyculin A, neither agent had any effect on thapsigargin-induced Ca²⁺ mobilization in 3T3-L1 preadipocytes. Therefore, neither the conformational coupling model nor the vesicular fusion model seems to be involved in SOCE in 3T3-L1 preadipocytes. On the other hand, the diffusible messenger model is more likely to occur in these cells. However, the conformational coupling model has been proposed based on research using

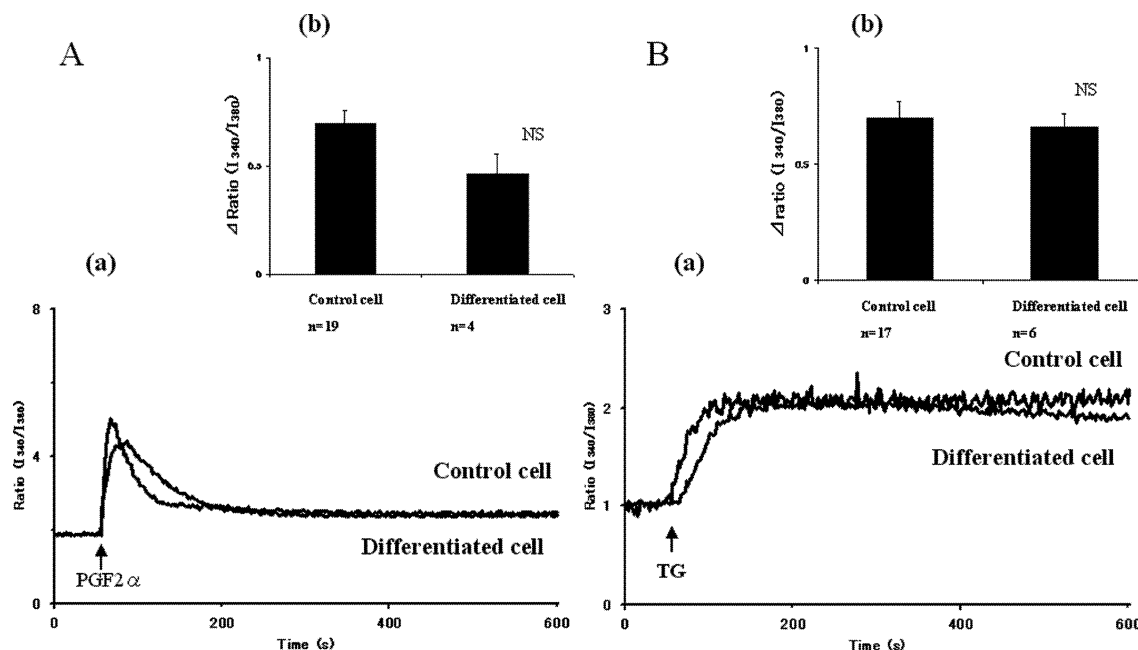


Fig. 7. PGF2 α - and thapsigargin-induced [Ca²⁺]_i mobilization in 3T3-L1 cells. A (a): Effect of PGF2 α on [Ca²⁺]_i mobilization in 3T3-L1 preadipocytes (control) and 3T3-L1 adipocytes (differentiated cells). Typical tracings are shown. A (b): The difference between the ratios of I340/I380 at 600 seconds and at the beginning of fluorescence determination. B (a): Effect of thapsigargin on [Ca²⁺]_i mobilization in 3T3-L1 preadipocytes (control) and 3T3-L1 adipocytes (differentiated cells). Typical tracings are shown. B (b): The difference between the ratios of I340/I380 at 600 seconds and at the beginning of fluorescence determination. Each value represents the mean \pm S.E.; NS, not significantly different.

several cell types, such as bovine adrenocortical cells and human platelets^{23,24}. This discrepancy might be caused by differences in cell types or cell lines. Therefore, different mechanisms should be considered whenever a SOCE channel is identified.

2. SOCE channels in 3T3-L1 cells

Some studies have indicated that *Drosophila* Trp and its mammalian homologues, TRPs, form subunits of Ca²⁺-permeable cation channels that mediate Ca²⁺ influx in response to activation of phospholipase C and internal Ca²⁺ store depletion by agonists^{19,20}. The TRP family can be divided into at least 6 subgroups: TRPCs, TRPVs, TRPMs, TRPA1, TRPPs, and TRPMLs²⁷⁻³⁰. Among these channels, TRPCs have previously been proposed to be regulated by the filling state of intracellular Ca²⁺ stores and are the elusive molecular candidates for SOCE³¹⁻³³. We detected TRPC mRNAs expressed in 3T3-L1 preadipocytes and found that mRNA for TRPC1 and TRPC2 were also expressed. Our results reveal the possible

involvement of TRPCs in SOCE on 3T3-L1 preadipocytes. While SOCE is high Ca²⁺-selective⁴, TRPCs are not Ca²⁺-selective, and other divalent ions, such as Sr²⁺, can pass through. In the presence of extracellular Sr²⁺ in place of extracellular Ca²⁺, thapsigargin-induced fura-2-fluorescence intensity in the plateau phase was reduced in 3T3-L1 preadipocytes. This finding indicates that TRPCs might not be involved in SOCE in 3T3-L1 preadipocytes.

Recently, stromal interacting molecule (STIM) 1 was identified as an adhesion molecule present in bone marrow stromal cells, and it was hypothesized that this protein might regulate cell formation³⁴. STIM1 has an EF-hand Ca²⁺-binding domain in the luminal site of the ER^{35,36}. Recent studies with short interfering (si)RNA have shown that STIM1 is involved in SOCE activity and functions as a Ca²⁺ sensor^{37,38}. On the other hand, Fesk et al. have designated Orail/CRACM1 as a SOCE regulator. They identified Orail by using a genome-wide RNA interference screen in *Drosophila* and a modified linkage of gene

mutation analysis in families with severe combined immune deficiency³⁹. Vig et al. have identified CRACM1 by means of RNA interference in *Drosophila*⁴⁰. The latest reports have demonstrated that STIM1 and Orai1/CRACM1 are essential components of SOCE⁴¹⁻⁴³. In a preliminary study, we detected the mRNA of STIM1 in 3T3-L1 preadipocytes (data not shown). Recently, Graham et al. reported the participation of STIM1 in the regulation of preadipocyte differentiation⁴⁴. We hope to determine whether expression of STIM1 and Orai1/CRACM1 is involved in the differentiation of 3T3-L1 preadipocytes.

Although we have shown that SOCE is the major $[Ca^{2+}]_i$ mobilization system in 3T3-L1 preadipocytes, whether $[Ca^{2+}]_i$ mobilization by SOCE is related to adipocyte differentiation remains unclear. Shi et al. have demonstrated the relationship between $[Ca^{2+}]_i$ mobilization and differentiation in human adipose tissue²¹. They have reported that the increase in $[Ca^{2+}]_i$ during the early stage of differentiation inhibits adipogenesis while the increase in $[Ca^{2+}]_i$ during the later stage of differentiation activates adipogenesis. Under our experimental conditions, thapsigargin-induced Ca^{2+} influx did not differ between 3T3-L1 adipocytes and preadipocytes. The SOCE mechanism itself might be an unchangeable system in 3T3-L1 cells during adipocyte differentiation.

PGF α activates phospholipase C through the FP receptor resulting in IP₃-stimulated Ca^{2+} -release from the ER^{9,10}. PGF 2α -induced SOCE activity in 3T3-L1 preadipocytes does not differ from that in differentiated cells. PGF 2α production has been reported to decrease during adipocyte differentiation^{45,46}. The levels of FP receptor do not change during adipocyte differentiation in 3T3-L1 cells⁴⁵. In addition, PGF 2α receptor regulatory protein (FPRP) has been identified as a transmembrane protein that inhibits binding of the FP receptor to its ligand⁴⁷. FPRP is not present in preadipocytes but it is induced during adipocyte differentiation in 3T3-L1 cells⁴⁸. Our results and those of previous reports suggest that SOCE activation through PGF 2α might be involved in adipogenesis in 3T3-L1 cells and that the regulation of endogenous PGF 2α production and FPRP levels, not

FP receptor levels, play important roles in the adipocyte differentiation of 3T3-L1 cells into adipocytes. Further studies are needed to clarify this possibility in 3T3-L1 cells.

REFERENCES

1. Berridge MJ, Lipp P, Bootman MD. The versatility and universality of calcium signalling. *Nat Rev Mol Cell Biol* 2000 ; 1 : 11-21.
2. Nakada MT, Stadel JM, Crooke ST. Mobilization of extracellular Ca^{2+} by prostaglandin F₂ alpha can be modulated by fluoride in 3T3-L1 fibroblasts. *Biochem J* 1990 ; 272 : 167-74.
3. Casimir DA, Miller CW, Ntambi JM. Preadipocyte differentiation blocked by prostaglandin stimulation of prostanoid FP₂ receptor in murine 3T3-L1 cells. *Differentiation* 1996 ; 60 : 203-10.
4. Parekh AB, Penner R. Store depletion and calcium influx. *Physiol Rev* 1997 ; 77 : 901-30.
5. Grynkiewicz G, Poenie M, Tsien RY. A new generation of Ca^{2+} indicators with greatly improved fluorescence properties. *J Biol Chem* 1985 ; 260 : 3440-50.
6. Tang S, Morgan KG, Parker C, Ware JA. Requirement for protein kinase C theta for cell cycle progression and formation of actin stress fibers and filopodia in vascular endothelial cells. *J Biol Chem* 1997 ; 272 : 28704-11.
7. Tirupathi C, Freichel M, Vogel SM, Paria BC, Mehta D, Flockerzi V, et al. Impairment of store-operated Ca^{2+} entry in TRPC4 (-/-) mice interferes with increase in lung microvascular permeability. *Circ Res* 2002 ; 91 : 70-6.
8. Wang J, Shimoda LA, Sylvester JT. Capacitative calcium entry and TRPC channel proteins are expressed in rat distal pulmonary arterial smooth muscle. *Am J Physiol Lung Cell Mol Physiol* 2004 ; 286 : L848-58.
9. Sakamoto K, Ezashi T, Miwa K, Okuda-Ashitaka E, Houtani T, Sugimoto T, et al. Molecular cloning and expression of a cDNA of the bovine prostaglandin F₂ alpha receptor. *J Biol Chem* 1994 ; 269 : 3881-6.
10. Abramovitz M, Boie Y, Nguyen T, Rushmore TH, Bayne MA, Metters KM, et al. Cloning and expression of a cDNA for the human prostanoid FP receptor. *J Biol Chem* 1994 ; 269 : 2632-6.
11. Thastrup O, Dawson AP, Scharff O, Foder B, Cullen PJ, Drøbak BK, et al. Thapsigargin, a novel molecular probe for studying intracellular calcium release and storage. *Agents Actions* 1989 ; 27 : 17-23.
12. Maruyama T, Kanaji T, Nakade S, Kanno T, Mikoshiba K. 2APB, 2-aminoethoxydiphenyl borate, a membrane-penetrable modulator of Ins(1,4,5)P₃-induced Ca^{2+} release. *J Biochem* 1997 ; 122 : 498-505.
13. Zweifach A, Lewis RS. Calcium-dependent potentiation of store-operated calcium channels in T

- lymphocytes. *J Gen Physiol* 1996; 107: 597-610.
14. Putney JW Jr., Broad LM, Braun FJ, Lievreumont JP, Bird GS. Mechanisms of capacitative calcium entry. *J Cell Sci* 2001; 114: 2223-9.
 15. Cooper JA. Effects of cytochalasin and phalloidin on actin. *J Cell Biol* 1987; 105: 1473-8.
 16. Shinoki N, Sakon M, Kambayashi J, Ikeda M, Oiki E, Okuyama M, et al. Involvement of protein phosphatase-1 in cytoskeletal organization of cultured endothelial cells. *J Cell Biochem* 1995; 59: 368-75.
 17. Hosoya N, Mitsui M, Yazama F, Ishihara H, Ozaki H, Karaki H, et al. Changes in the cytoskeletal structure of cultured smooth muscle cells induced by calyculin-A. *J Cell Sci* 1993; 105: 883-90.
 18. Patterson RL, van Rossum DB, Gill DL. Store-operated Ca^{2+} entry: evidence for a secretion-like coupling model. *Cell* 1999; 98: 487-99.
 19. Birnbaumer L, Zhu X, Jiang M, Boulay G, Peyton M, Vannier B, et al. On the molecular basis and regulation of cellular capacitative calcium entry: roles for Trp proteins. *Proc Natl Acad Sci USA* 1996; 93: 15195-202.
 20. Montell C, Rubin GM. Molecular characterization of the *Drosophila* *trp* locus: a putative integral membrane protein required for phototransduction. *Neuron* 1989; 2: 1313-23.
 21. Shi H, Halvorsen YD, Ellis PN, Wilkison WO, Zemel MB. Role of intracellular calcium in human adipocyte differentiation. *Physiol Genomics* 2000; 3: 75-82.
 22. Berridge MJ. Capacitative calcium entry. *Biochem J* 1995; 312: 1-11.
 23. Kawamura M, Terasaka O, Ebisawa T, Kondo I, Masaki E, Ahmed A, et al. Integrity of actin-network is involved in uridine 5'-triphosphate evoked store-operated Ca^{2+} entry in bovine adrenocortical fasciculata cells. *J Pharmacol Sci* 2003; 91: 23-33.
 24. Redondo PC, Harper AG, Salido GM, Pariente JA, Sage SO, Rosado JA. A role for SNAP-25 but not VAMPs in store-mediated Ca^{2+} entry in human platelets. *J Physiol* 2004; 558: 99-109.
 25. Rosado JA, Sage SO. A role for the actin cytoskeleton in the initiation and maintenance of store-mediated calcium entry in human platelets. *Trends Cardiovasc Med* 2000; 10: 327-32.
 26. Smani T, Zakharov SI, Csutura P, Leno E, Trepakova ES, Bolotina VM. A novel mechanism for the store-operated calcium influx pathway. *Nat Cell Biol* 2004; 6: 113-20.
 27. Montell C, Birnbaumer L, Flockerzi V. The TRP channels, a remarkably functional family. *Cell* 2002; 108: 595-8.
 28. Wissenbach U, Niemeyer BA, Flockerzi V. TRP channels as potential drug targets. *Biol Cell* 2004; 96: 47-54.
 29. Montell C, Birnbaumer L, Flockerzi V, Bindels RJ, Bruford EA, Caterina MJ, et al. A unified nomenclature for the superfamily of TRP cation channels. *Mol Cell* 2002; 9: 229-31.
 30. Pedersen SF, Owsianik G, Nilius B. TRP channels: an overview. *Cell Calcium* 2005; 38: 233-52.
 31. Hardie RC, Minke B. Novel Ca^{2+} channels underlying transduction in *Drosophila* photoreceptors: implications for phosphoinositide-mediated Ca^{2+} mobilization. *Trends Neurosci* 1993; 16: 371-6.
 32. Philipp S, Cavalié A, Freichel M, Wissenbach U, Zimmer S, Trost C, et al. A mammalian capacitative calcium entry channel homologous to *Drosophila* TRP and TRPL. *EMBO J* 1996; 15: 6166-71.
 33. Zitt C, Zobel A, Obukhov AG, Harteneck C, Kalkbrenner F, Lückhoff A, et al. Cloning and functional expression of a human Ca^{2+} -permeable cation channel activated by calcium store depletion. *Neuron* 1996; 16: 1189-96.
 34. Oritani K, Kincaid PW. Identification of stromal cell products that interact with pre-B cells. *J Cell Biol* 1996; 134: 771-82.
 35. Williams RT, Manji SS, Parker NJ, Hancock MS, Van Stekelenburg L, Eid JP, et al. Identification and characterization of the STIM (stromal interaction molecule) gene family: coding for a novel class of transmembrane proteins. *Biochem J* 2001; 357: 673-85.
 36. Manji SS, Parker NJ, Williams RT, van Stekelenburg L, Pearson RB, Dziadek M, et al. STIM1: a novel phosphoprotein located at the cell surface. *Biochim Biophys Acta* 2000; 1481: 147-55.
 37. Liou J, Kim ML, Heo WD, Jones JT, Myers JW, Ferrell JE Jr., et al. STIM is a Ca^{2+} sensor essential for Ca^{2+} -store-depletion-triggered Ca^{2+} influx. *Curr Biol* 2005; 15: 1235-41.
 38. Roos J, DiGregorio PJ, Yeromin AV, Ohlsen K, Lioudyno M, Zhang S, et al. STIM1, an essential and conserved component of store-operated Ca^{2+} channel function. *J Cell Biol* 2005; 169: 435-45.
 39. Feske S, Gwack Y, Prakriya M, Srikanth S, Puppel SH, Tanasa B, et al. A mutation in Orai1 causes immune deficiency by abrogating CRAC channel function. *Nature* 2006; 441: 179-85.
 40. Vig M, Peinelt C, Beck A, KooMOA DL, Rabah D, Koblan-Huberson M, et al. CRACM1 is a plasma membrane protein essential for store-operated Ca^{2+} entry. *Science* 2006; 312: 1220-3.
 41. Mercer JC, Dehaven WI, Smyth JT, Wedel B, Boyles RR, Bird GS, et al. Large store-operated calcium selective currents due to co-expression of Orai1 or Orai2 with the intracellular calcium sensor, Stim1. *J Biol Chem* 2006; 281: 24979-90.
 42. Soboloff J, Spassova MA, Tang XD, Hewavitharana T, Xu W, Gill DL. Orai1 and STIM reconstitute store-operated calcium channel function. *J Biol Chem* 2006; 281: 20661-5.
 43. Putney JW Jr. New molecular players in capacitative Ca^{2+} entry. *J Cell Sci* 2007; 120: 1959-65.
 44. Graham SJ, Black MJ, Soboloff J, Gill DL, Dziadek MA,

- Johnstone LS. Stim1, an endoplasmic reticulum Ca^{2+} sensor, negatively regulates 3T3-L1 pre-adipocyte differentiation. *Differentiation* 2009 ; 77 : 239-47.
45. Miller CW, Casimir DA, Ntambi JM. The mechanism of inhibition of 3T3-L1 preadipocyte differentiation by prostaglandin F2alpha. *Endocrinology* 1996 ; 137 : 5641-50.
46. Hyman BT, Stoll LL, Spector AA. Prostaglandin production by 3T3-L1 cells in culture. *Biochim Biophys Acta* 1982 ; 713 : 375-85.
47. Orlicky DJ. Negative regulatory activity of a prostaglandin F2 alpha receptor associated protein (FPRP). *Prostaglandins Leukot. Essent. Fatty Acids* 1996 ; 54 : 247-59.
48. Orlicky DJ, Lieber JG, Morin CL, Evans RM. Synthesis and accumulation of a receptor regulatory protein associated with lipid droplet accumulation in 3T3-L1 cells. *J Lipid Res* 1998 ; 39 : 1152-61.